Nanoscale

Accepted Manuscript

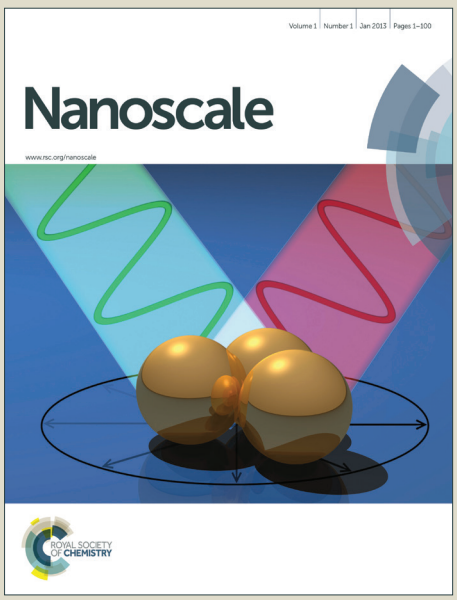

ROYAL SOCIETY OF CHEMISTRY

www.rsc.org/nanoscale

Journal Name

ARTICLE

Pollutant capturing SERS substrate: Porous boron nitride microfibers with uniform silver nanoparticles decoration

Received 00th January 20xx,
Accepted 00th January 20xx

DOI: 10.1039/x0xx00000x

www.rsc.org/

Pengcheng Dai,†*[a,b] Yanming Xue,†*[b] Xuebin Wang,[b] Qunhong Weng,[b] Chao Zhang,[b] Xiangfen Jiang,*[b] Daiming Tang,[b] Xi Wang,[b] Naoyuki Kawamoto,[b] Yusuke Ide,[b] Masanori Mitome,[b] Dmitri Golberg,*[b] and Yoshio Bando[b]

How to concentrate target molecules on the surface of SERS substrate is a key problem toward the practical application of SERS. Herein, we designed for the first time a pollutant capturing surface enhanced Raman spectroscopy (SERS) substrate, namely porous BN microfibers with uniform Ag nanoparticles decoration, in which BN microfibers adsorb pollutants, while Ag nanoparticle provide a SERS activity. This SERS substrate captures pollutants from an aqueous solution completely and accumulates them all on its surface without introducing noisy signals. The pores of BN pretects the silver particles from aggregation and enables BN/Ag a stable and recyclable SERS substrate. What' more, while the dyes are thoroughly concentrated from a diluted solution, the SERS detection limit is easily enhanced, from 10^{-6} M to 10^{-9} M.

1. Introduction

Water pollution is a leading cause of diseases and deaths all over the world, which requires ongoing evolution on both pollutant detection and clearance.[1-3] The first and most crucial emphasis toward water pollution is, identifying the pollutants in water fleetly, even though the concentration is relatively low.[3-5] Among all the detecting methods, surface enhanced Raman spectroscopy (SERS) has attracted numerous research interest in the field of chemical and biochemical analytics.[6-12] However, traditional SERS substrate is mainly based on metal nanostructures, such as Ag and Au, whose surface is hydrophilic[6, 8, 13]. They are sensitive to molecules with thiol (-SH) and amino (-NH_2), which could easily connect to the surface of Ag or Au, but lack of sensitivity to most of other water pollutants.[14] The intensity of SERS signal highly depends on the amount of molecules on the surface.[15, 16] Therefore, how to concentrate target molecules on the near surface of SERS active substrate has become a critical challenge.

Traditionally, surface modifications with organic molecules such as cyclodextrin[17], alkanethiols[18], et. al., are applied to attract target molecules, which leads to another drawback: modifiers generate misleading signals.[19] It is challenging to modify SERS-active substrates using conventional nonfouling materials without introducing interference from their SERS signals. We present in this work a new design namely pollutant capturing SERS substrate: forming an inorganic pollutant capturer whose surface has uniform silver nanoparticles decoration, in which inorganic pollutant capturer adsorbs pollutants and concentrates them without generate noisy signals, while silver nanoparticles provide a SERS activity. One challenging issue for this design is to find a suitable inorganic substrate with ignorable SERS signal and excellent adsorptive activity. Among all the alternatives, light-weight boron nitride (BN) nanostructures were noticed as the promising substances due to their high thermal stability, high resistance to oxidation, chemical inertness[20, 21], and most importantly, superior absorbing performances.[22-24] Their high surface areas make them valuable for efficient adsorption of various pollutants, for instance, organics, heavy metal ions, and gases. [25, 26] Comparing with organic ligands, BN nanostructures have ignorable Raman signal.[23, 27] What's more, Zhang et al., reported that the presence of BN leads to enhancement of SERS signal.[28]

Herein, we report the design and synthesis of a novel pollutant capturing SERS substrate based on boron nitride microfibers uniformly decorated with silver nanoparticles (BN/Ag). BN/Ag captures the pollutants without introducing any disturbing signals and also reveals good SERS activity. While the dyes are thoroughly concentrated from a diluted solution, the SERS detection limit is easily enhanced, from 10^{-6} M to 10^{-9} M, by simply adding more solution. When loaded on a filtering paper, the BN/Ag membrane could efficiently concentrate dyes through suction and provide SERS signals as well. We believe that this novel pollutant capturing SERS substrate is an important step toward effective and practical environmental water analysis.

[a] Research Institute of Unconventional Petroleum and Renewable Energy, China University of Petroleum (East China), Qingdao 266580, P. R. China
[b] International Center for Materials Nanoarchitectonics (WPI-MANA), National Institute for Materials Science (NIMS) Namiki 1-1, Tsukuba, Ibaraki, 305-0044, Japan
† These authors contributed equally to this work
Electronic Supplementary Information (ESI) available: [details of any supplementary information available should be included here]. See DOI: 10.1039/x0xx00000x

2. Experimental Section

2.1. Preparation of BN microfibers

2.52 g melamine ($C_3N_6H_6$, 99.5%, Wako Pure Chemical Industries, Ltd.) and 2.47 g boric acid (H_3BO_3, 99.5%, Sigma-Aldrich CO., LTD.) at a molar ratio of 1:2 were dissolved into 500 ml deionized water and held at 90 °C. Once the solution became transparent, it was cooled to room temperature. As a result, the flocculent precipitate ($C_3N_6H_6{\cdot}2H_3BO_3$, namely, M·2B) was immediately formed in the cooled solution. After further filtering and drying, the fiber-like M·2B was obtained. Finally, uniform-morphology BN fibers were formed via high-temperature pyrolyzation of M·2B at 1000 °C under a constant ammonia flow of 100 ml/min for 3 h.

2.2. Preparation of Ag nanoparticle decorated BN microfibers

40 mg BN microfibers were dispersed in 200 ml $AgNO_3$ ethanol solution (0.1 M) and stirred overnight. The precipitate was filtered out and dried at 60 °C. Afterward, it was transferred into a tube furnace and heated at 450 °C for 2 h under a constant argon flow of 100 ml/min. Finally, the yellow powder (BN/Ag) was cleaned with ethanol and dried. To prepare BN/Ag membrane, 5 mg BN/Ag was dispersed in 50 ml DI water and carefully filtered on a microfiltration membrane. The as prepared membrane was used in situ as a pollutant capturing SERS substrate.

2.3. Preparation of Ag nanoparticles

Ag nanoparticles was prepared according to ref 29.[29] Generally, silver nitrate (9 mg) was dissolved in water/glycerol solution (40 vol% glycerol, 50 ml, 95 °C), followed by adding 1 mL sodium citrate solution (3%) and one hour heating constantly at 95 °C.

2.4. Characterization

The morphology and structure of samples were analyzed on JSM-6700 SEM and JEM-3000F HRTEM (300 kV). XRD patterns were recorded using a Rigaku Ultima III (Cu Kα) diffractometer. UV-Vis spectra were taken on a JASCO V-570 UV/VIS/NIR spectrophotometer. Raman spectra were collected on a Horiba Jobin-Yvon T6400 Raman system with a 514.5 nm excitation laser. The laser intensity was 10 mW with an accumulation time of 5 s for each spectrum. Backgrounds of the Raman spectra were subtracted before plotting. Chemical state characterizations were carried out using an XPS spectrometer (PHI Quantera SXM).

3. Result and Discussion

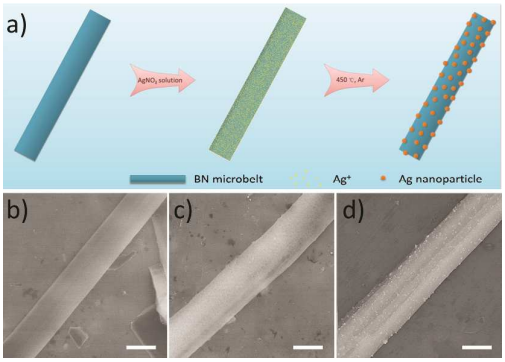

Fig. 1. a) Schematic illustration of the preparation of BN microfibers modified with Ag nanoparticles. b), c), d) SEM images of the BN microfiber, BN microfiber with Ag^+ and BN microfiber decorated with Ag nanoparticles. The scale bars are 1 μm.

BN/Ag was prepared via a facile three-step approach (Fig. 1a). Firstly, BN microfibers were synthesized as reported previously[30] (Fig. 1b). Secondly, BN microfibers were dispersed into $AgNO_3$ ethanol solution under stirring overnight. As confirmed by XPS (Fig. S1), the surface of BN microfibers is coated with –OH, –NH–, and $–NH_2$ groups, which are easily coordinated with Ag cations. Therefore, Ag cations were absorbed on BN microfibers' surfaces without forming any particles (Fig. 1c, Fig. S2). Afterward, the BN microfibers were filtered out and dried, followed by the annealing process at 400 °C for 30 min under argon atmosphere. At such temperature, the absorbed Ag salt decomposed and generated Ag nanoparticles (Fig. 1d, Fig. S3). The uniform cation adsorption led to uniform Ag nanoparticle coverage on the BN microfibers (Fig. 1d).

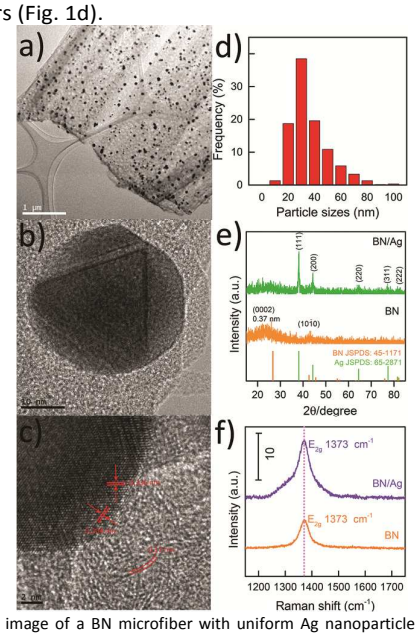

Fig. 2 a) TEM image of a BN microfiber with uniform Ag nanoparticle decoration; b) TEM image of a typical Ag nanoparticle on the surface of BN microfiber. c) HRTEM image of the interface between BN microfiber and Ag nanoparticle. d) Size distribution of Ag nanoparticles (600 nanoparticles are counted). e) X-ray diffraction patterns of BN microfibers and Ag nanoparticle-decorated BN microfibers. Standard spectra of BN and Ag are shown in the bottom[31, 32]. f) Raman spectra of BN microfibers and Ag nanoparticle-decorated BN microfibers.

As shown in Fig. 2a, Ag nanoparticles, whose size ranges from 10 to 100 nm and peaks at 30 nm (Fig. 2d), are randomly distributed on BN microfiber's surfaces. TEM studies (Fig. 2b and Fig. S5) also reveal that the as-grown Ag polycrystalline nanoparticles are randomly shaped. Fig. 2c shows the edge of an Ag nanoparticle on the individual BN microfiber. The marked interplanar d-spacings of 0.236 nm and 0.204 nm match well with the (111) and (200) lattice distances in silver. The lattice fringes with d-spacing of 0.37 nm belong to the (0002) plane of the BN microfiber[23], and correspond well with the XRD data in Fig. 2e, in which two weak and wide peaks at 2θ = ~24 and 43° are assigned to the (0002) and (10$\bar{1}$0) planes of hexagonal BN. An XRD pattern collected from the Ag-decorated BN microfibers (BN/Ag) revealed the typical (111), (200) (220) (311) and (222) reflections at 2θ = 38.1, 44.3, 64.4, 77.4 and 81.5°, correspondingly, which further confirmed the presence of FCC Ag.[32] Fig. 2e shows the Raman spectra of BN microfibers and BN/Ag samples. The peak at 1373 cm^{-1} corresponds to the E_{2g} vibration peak of hexagonal BN.[23] After Ag decoration, there is still one peak at 1373 cm^{-1}, relating to the E_{2g} vibration hexagonal BN. This is because silver doesn't have a Raman signal. And the peak intensity of BN/Ag is as low as 11 counts, which is ignorable and would not introduce interference peaks.

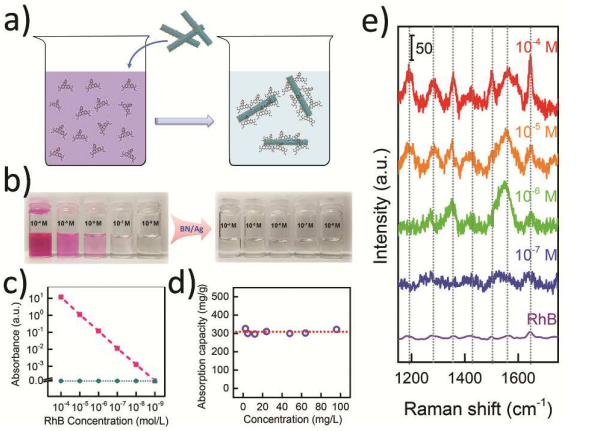

Fig. 3 a) Schematic illustration showing the adsorption of RhB from an aqueous solution by a BN/Ag hybrid material. b) Photos showing that RhBs were totally captured from the solution. c) UV-vis spectra of RhB solution before (pink) and after (blue) BN/Ag adsorption. d) Adsorption capacity of BN/Ag with different RhB concentrations. e) Raman spectra of RhB (10^{-4} M×2 ml, 10^{-5} M×2 ml, 10^{-6} M×2 ml, 10^{-7} M×2 ml and RhB powder) adsorbed on BN/Ag (2 mg).

Once prepared, BN/Ag is ready to serve as a pollutant capturing SERS substrate. Rhodamine B (RhB), a common hydrosoluble dye, was chosen as the target molecule for adsorption and SERS sensing. With a surface area of 670 m^2/g (Fig. S7), BN/Ag exhibits relatively high adsorbing activity. As schemed in Fig. 3a, BN/Ag could capture all the molecules irreversibly from an aqueous solution and enrich all target molecules on its surface. The maximum adsorption capacity is 307.8 mg/g in average, as seen in Fig. 3d. Inside the adsorption range, all RhB molecules are adsorbed by the BN/Ag which results in the complete fading of the pink RhB solution after adsorption (Fig. 3b). UV-vis absorption spectroscopy was used to identify the concentration before and after adsorption. RhB has a specific absorption peak at 552 nm in UV-vis spectra, whose detection limit during employed UV-vis spectroscopy is ~ 10^{-8} M, as shown in Fig. S8. The absorbance of RhB (10^{-4} M, 10^{-5} M, 10^{-6} M, 10^{-7} M, 10^{-8} M and 10^{-9} M) before and after adsorption is shown in Fig. 3c. After the adsorption, the peak in 552 nm completely disappeared (Fig. S9), which indicates that RhB is totally removed from water.

The SERS spectra of RhB on BN/Ag were measured under continuous laser radiation (10 mW) in air by Raman spectroscopy. Apparently, the adsorption of RhB molecules on BN/Ag enhanced the Raman response by several orders of magnitude, as illustrated in Fig. 3d. The characteristic peaks located at 1195 cm^{-1}, 1275 cm^{-1}, 1350 cm^{-1}, 1430 cm^{-1}, 1560 cm^{-1} and 1650 cm^{-1}, are in a good agreement with the Raman spectra of RhB powder and the literature data.[33] Well-resolved Raman signatures of RhB at 10^{-4} M, 10^{-5} M and 10^{-6} M could be readily observed, while the signal of RhB with a concentration of 10^{-7} M is too weak to be identified. Therefore, the detection limit is defined as 10^{-6} M, which is comparable to the previous reports. The analytical SERS enhancement factor (EF)[34] was estimated using the equation $EF = I_{SERS}N_{NR}/I_{NR}N_{surface}$, to be on the order of 10^6 by comparing the SERS spectrum with the regular Raman spectrum of a bulk RhB sample on glass substrate, where I_{SERS} represents the SERS intensity of the 1650 cm^{-1} band for RhB adsorbed on BN/Ag; and I_{NR} represents the normal Raman intensity recorded for RhB on a glass substrate. N_{SERS} and N_{NR} represent the corresponding average number of molecules of RhB on BN/Ag and glass.

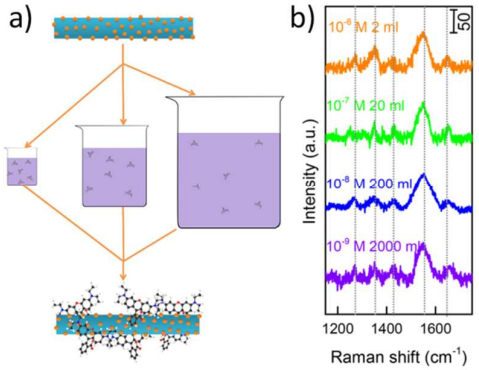

Fig. 4 a) Schematics showing that solutions with the same amount of RhB result in the same $N_{surface}$. b) Raman spectra of the solutions with the same amount of RhB but at different concentration and volumes.

Converted from the equation $EF=I_{SERS}N_{NR}/I_{NR}N_{surface}$, another equation $I_{SERS}= EF \cdot I_{NR}N_{surface}/N_{NR}$ can be obtained. For the same SERS substrate (BN/Ag) and target molecule (RhB), EF, I_{NR} and $N_{surface}$ are constants. Therefore, the intensity of SERS signal (I_{SERS}) only relates to the amount of RhB molecules on BN/Ag ($N_{surface}$). Since BN/Ag could totally capture the target molecules from water, we can obtain enough RhB molecules on BN/Ag by simply increasing the volume of RhB solution with ultralow concentration ($N_{SERS} = c_{RhB}V$), so that RhB solution, whose concentration is even below 10^{-6} M, can still provide intense Raman signal. Thus, we put the same amount (2 mg) of BN/Ag into different volumes of low concentration

solutions. Fig. 4b depicts the SERS signal of RhB on BN/Ag from RhB solution of 10^{-6} M×2 ml, 10^{-7} M×20 ml, 10^{-8} M×200 ml, and 10^{-9} M×2000 ml. Unlike the Raman spectra of 10^{-7} M×2 ml, whose signal is too weak to be seen, 10^{-7} M×20 ml, 10^{-8} M×200 ml and 10^{-9} M×2000 ml show similarly intense SERS signals as 10^{-6} M×2 ml, which implies that these samples have similar $N_{surface}$. The same outcome was also obtained using methylene blue (MB) as a target molecule (Fig. S10). Thus, by simply enlarging the volume of a solution with ultralow concentration, the detection limit is easily improved from 10^{-6} M to 10^{-9} M.

The separated contribution of BN and Ag is proven by comparing the adsorption capacities and SERS activities of bare BN microfiber, bare Ag nanoparticles (NPs) and BN/Ag. As shown in Fig. S12, BN microfibers show high adsorption capacity (431 mg/g) but have no SERS activity, while bare Ag NPs show good SERS activity but exhibit quite low adsorption capacity (0.43 mg/g). Therefore, the adsorbing activity is mainly contributed by BN microfibers and the SERS activity is provided by Ag NPs.

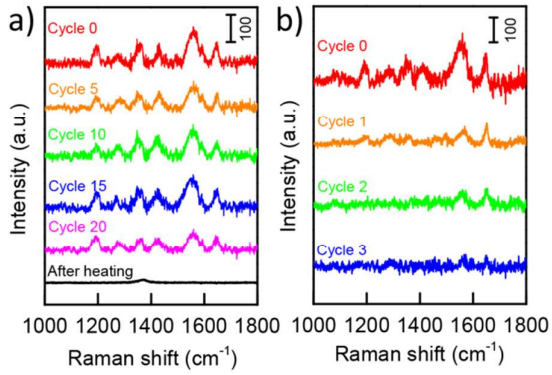

Fig. 5 a) Raman spectra of RhB (10^{-5} M) on BN/Ag substrate during 20 cycles of recyclability test. A typical Raman spectrum of BN/Ag after heating at 400 °C to remove RhB is shown in the bottom for comparison. b) Raman spectra of RhB (10^{-5} M) on Ag nanoparticle substrate during reusability test.

The recyclability of BN/Ag SERS substrate was concerned as well. Burning off in air is the most simple and effective approach to remove dye molecules. Therefore, after SERS measurement, the substrate was heated at 400 °C for 5min to clean the adsorbed dye RhB. As shown in Fig. 5, no RhB signal was observed after heating, implying that RhB was effectively removed. The only peak at 1373 cm^{-1} is attributed to the Raman signal of BN. The regenerated BN/Ag was dispersed into RhB solution again to adsorb RhB molecules, followed by SERS measurement to fulfil a whole cycle. This heating and re-adsorbing process was repeated up to 20 times. As Fig. 5a shows, there is no obvious change in both peak position and intensity, implying excellent recyclability. As a control, the Raman signals using Ag NPs as SERS substrate almost disappeared after only 3 cycles.

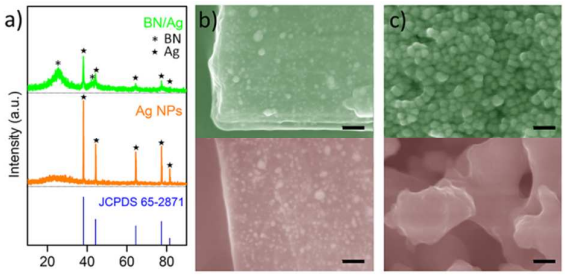

Fig. 6 a) XRD patterns of BN/Ag and Ag NPs after recyclability test, the standard signal of silver is shown in the bottom. b) and c) SEM images of BN/Ag and Ag NPs before (top) and after (bottom) recyclability measurement. The scale bar inserted is 100 nm.

The excellent reusability indicates good stability of BN/Ag. After recyclability measurement at 400 °C, the XRD pattern of BN/Ag (Fig. 6a) is the same with the original one in Fig. 2e. Signals of both BN and Ag are easily found in the XRD pattern, while no impurity signal such as Ag_2O is found, implying that BN/Ag has good resistance to thermal oxidation. It is notable that Ag NPs were not oxidized as well. However, Ag NPs aggregated into big particles whose sizes are larger than 500 nm during the annealing process (Fig. 6c), which leads to the decrease of SERS signals[35]. Even loaded on BN nanosheets, the aggregation of Ag NPs is still a problem.[21] Using porous BN microfibers as supporting substrate solved this problem perfectly. In addition to loading on the surface of BN microfibers, there are lots of Ag NPs decorated inside the pores of BN microfibers. The limited pore size restricted the Ag NPs from moving around and aggregating into larger particles. Therefore, both the size and distribution of BN/Ag remain unchanged after thermal treatment.

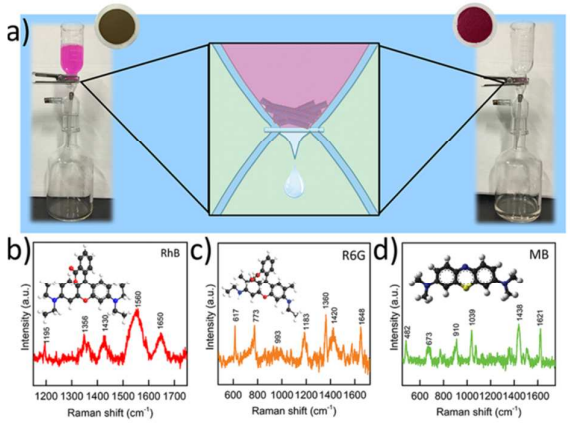

Fig. 7 a) Scheme showing the filtration and adsorption process of a BN/Ag membrane. Digital images of BN/Ag membranes before and after adsorption are inserted as well. b), c), and d) SERS signals of RhB, R6G and MB (10^{-6} M).

Finally, we demonstrate that the BN/Ag aggregates could be loaded onto a filter membrane and act as a membrane for rapid pollutant capture and SERS detection. As a surface-sensitive technique, SERS performance is highly related to the distance between the target molecules and SERS active material.[15] Therefore, the target molecules must be placed at the hot spots, where they can be efficiently detected. Commonly, two methods are used to place the target

molecules. One is dropping the solution onto a SERS substrate, followed by drying process. Under this dropping method, the substrate could accommodate very little amount of solution. Therefore, the detection limit is usually high and is difficult to be improved further. The other method is dipping the substrate into the solution for a certain time. The target molecules are adsorbed on the substrate surface. However, the adsorptions are usually reversible, which have a sort of equilibrium, so that only a part of the molecules is adsorbed. Moreover, it generally takes up to several hours to enrich samples using this immersion method.[14, 17] Since BN/Ag could capture the pollutants rapidly, fabricating them into a membrane can easily be accomplished to effectively concentrate the molecules via simple filtering. As Fig. 7a shows, RhB is adsorbed by BN/Ag while it passes through the membrane under pumping. The solution becomes transparent after filtering, which indicates that RhB has fully been captured and concentrated on the surface of the BN/Ag membrane. Three Raman active agents, namely, RhB, methylene blue and rhodamine 6G, were chosen for the final validation of the sensing system. Fig. 7b-d displays the Raman spectra of RhB (10^{-6} M×50 ml), methylene blue (MB, 10^{-6} M×50 ml) and rhodamine 6G (R6G, 10^{-6} M×50 ml) using a BN/Ag membrane fabricated by 5 mg of the BN/Ag material. All these dyes show corresponding SERS peaks, as reported[33, 36, 37], indicating that the present BN/Ag membrane is an excellent capturing SERS substrate for variety of organic pollutants. BN/Ag is easily peeled off from the filtering paper by sonication in water followed by heating in air to remove dye molecules. The regenerated BN/Ag can be reloaded on filtering paper again for reuse. Since dye molecules are adsorbed homogeneously in aqueous solution, the homogeneity of the SERS is quite good. As shown in Fig. S11a, SERS signals of 10 different sports on the membrane shows no obvious difference. After 10-cycles regeneration, the Raman spectra show no obvious change comparing with the original one except the slight intensity drop (Fig. S11b), indicating good repeatability and homogeneity of the SERS performances.

Conclusions

In summary, we demonstrated a facile approach that can produce a uniform Ag nanoparticle coverage on porous BN microfibers. The employment of porous BN microfibers with enables BN/Ag a sensitive, stable and recyclable capturing SERS substrate. This work addresses the important issue peculiar to SERS. Often, the target molecules are needed to be attached on the surface of Ag by means of organic modifiers spoiling the quality of Raman spectra. By contrast, our work documents that an inorganic pollutant capturer is more efficient and generate no disturbing Raman signals. By simply feeding more pollutant solution, the SERS detection limit of BN/Ag could be improved by at least three orders of magnitude. While there are still more effort needed in terms of quantitative analysis and selectivity, the present work opens the new pathway toward making high-sensitivity SERS substrates for rapid analyses of environmental water samples.

Acknowledgements

This work was funded by the World Premier International Center for Materials Nanoarchitectonics (WPI-MANA) of NIMS, Tsukuba, Japan and KAKENHI Program (15K18216) of Japan Society for the Promotion of Science (JSPS).

References

1. S. D. Faust and O. M. Aly, *Adsorption Processes for Water Treatment*, Butterworth, London, 1987.
2. J. Crittenden, R. Trussell, D. Hand, K. Howe and G. Tchobanoglous, *Water Treatment: Principles and Design*, John Wiley & Sons, Hoboken, 2005.
3. E. W. Rice, R. B. Baird, A. D. Eaton and L. S. Clesceri, *Standard Methods for the Examination of Water and Wastewater*, American Water Works Association/American Public Works Association/Water Environment Federation, New York, 1998.
4. I. Gupta, A. Kumar, C. Singh and R. Kumar, *Journal of Geographic Information System*, 2015, **07**, 71-84.
5. C. Liu, X. Zhang, L. Li, J. Cui, Y. E. Shi, L. Wang and J. Zhan, *The Analyst*, 2015, **140**, 4668-4675.
6. B. Sharma, R. R. Frontiera, A.-I. Henry, E. Ringe and R. P. Van Duyne, *Materials Today*, 2012, **15**, 16-25.
7. E. C. Le Ru and P. G. Etchegoin, *Annu. Rev. Phys. Chem.*, 2012, **63**, 65-87.
8. N. J. Halas and M. Moskovits, *MRS Bulletin*, 2013, **38**, 607-611.
9. S. Schlucker, *Angew. Chem. Int. Ed.* , 2014, **53**, 4756-4795.
10. M. Fan, G. F. Andrade and A. G. Brolo, *Anal. Chim. Acta*, 2011, **693**, 7-25.
11. S. K. Cha, J. H. Mun, T. Chang, S. Y. Kim, J. Y. Kim, H. M. Jin, J. Y. Lee, J. Shin, K. H. Kim and S. O. Kim, *ACS Nano*, 2015, **9**, 5536–5543.
12. F. Sun, J.-R. Ella-Menye, D. D. Galvan, T. Bai, H.-C. Hung, Y.-N. Chou, P. Zhang, S. Jiang and Q. Yu, *ACS Nano*, 2015, **9**, 2668–2676.
13. P. L. Stiles, J. A. Dieringer, N. C. Shah and R. P. Van Duyne, *Annu. Rev. Anal. Chem.*, 2008, **1**, 601-626.
14. X. Jiang, M. Yang, Y. Meng, W. Jiang and J. Zhan, *ACS Appl. Mater. Interfaces*, 2013, **5**, 6902-6908.
15. B. L. Darby and E. C. Le Ru, *J. Am. Chem. Soc.*, 2014, **136**, 10965-10973.
16. A. Tripathi, E. D. Emmons, A. W. Fountain, J. A. Guicheteau, M. Moskovits and S. D. Christesen, *ACS Nano*, 2015, **9**, 584–593.
17. J. Yuan, Y. Lai, J. Duan, Q. Zhao and J. Zhan, *J. Colloid. Interface Sci.*, 2012, **365**, 122-126.
18. J. Du and C. Jing, *J. Phys. Chem. C*, 2011, **115**, 17829-17835.
19. Y. Lai, J. Cui, X. Jiang, S. Zhu and J. Zhan, *The Analyst*, 2013, **138**, 2598-2603.
20. Q. Weng, X. Wang, Y. Bando and D. Golberg, *Adv. Energy Mat.*, 2014, **4**, 1301525-1301533.
21. Y. Lin, C. E. Bunker, K. A. Fernando and J. W. Connell, *ACS Appl. Mater. Interfaces*, 2012, **4**, 1110-1117.
22. J. Li, X. Xiao, X. Xu, J. Lin, Y. Huang, Y. Xue, P. Jin, J. Zou and C. Tang, *Sci. Rep.*, 2013, **3**, 3208.
23. Q. Weng, X. Wang, C. Zhi, Y. Bando and D. Golberg, *ACS Nano*, 2013, **7**, 1558–1565.

24. W. Lei, D. Liu and Y. Chen, *Adv. Mater. Interfaces*, 2015, **2**, 1400529.
25. J. Li, J. Lin, X. Xu, X. Zhang, Y. Xue, J. Mi, Z. Mo, Y. Fan, L. Hu, X. Yang, J. Zhang, F. Meng, S. Yuan and C. Tang, *Nanotechnology*, 2013, **24**, 155603.
26. W. Lei, D. Portehault, D. Liu, S. Qin and Y. Chen, *Nat. Commun.*, 2013, **4**, 1777.
27. Q. Cai, L. H. Li, Y. Yu, Y. Liu, S. Huang, Y. Chen, K. Watanabe and T. Taniguchi, *Physical chemistry chemical physics : PCCP*, 2015, **17**, 7761-7766.
28. S. Yang, Z. Zhang, J. Zhao and H. Zheng, *Journal of Alloys and Compounds*, 2014, **583**, 231-236.
29. D. Steinigeweg and S. Schlucker, *Chem. Commun.*, 2012, **48**, 8682-8684.
30. Y. Xue, X. Jin, Y. Fan, J. Lin, J. Li, C. Ren, X. Xu, D. Liu, L. Hu, F. Meng, J. Zhang and C. Tang, *Int. J. Ploym. Mat. Polym. Biomat.*, 2014, **63**, 794-799.
31. L. Wang, L. Xu, C. Sun and Y. Qian, *J. Mater. Chem.*, 2009, **19**, 1989.
32. P. Hu and Y. Cao, *Dalton Trans.*, 2012, **41**, 8908-8912.
33. X. Liu, Y. Shao, Y. Tang and K. F. Yao, *Sci. Rep.*, 2014, **4**, 5835.
34. E. C. L. Ru, E. Blackie, M. Meyer and P. G. Etchegoin, *J. Phys. Chem. C*, 2007, **111**, 13794-13803.
35. X. Han, H. Wang, X. Ou and X. Zhang, *J. Mater. Chem.*, 2012, **22**, 14127.
36. G.-N. Xiao and S.-Q. Man, *Chem. Phys. Lett.*, 2007, **447**, 305-309.
37. J. Chen, T. Martensson, K. A. Dick, K. Deppert, H. Q. Xu, L. Samuelson and H. Xu, *Nanotechnology*, 2008, **19**, 275712.